Structural changes of ultrasonicated bovine serum albumin revealed by hydrogen–deuterium exchange and mass spectrometry

ARTICLE *in* ANALYTICAL AND BIOANALYTICAL CHEMISTRY · SEPTEMBER 2014

Impact Factor: 3.44 · DOI: 10.1007/s00216-014-8136-6 · Source: PubMed

Anal Bioanal Chem (2014) 406:7243–7251
DOI 10.1007/s00216-014-8136-6

RESEARCH PAPER

Structural changes of ultrasonicated bovine serum albumin revealed by hydrogen–deuterium exchange and mass spectrometry

Qiuting Zhang · Zongcai Tu · Hui Wang · Xiaoqin Huang · Xiaomei Sha · Hui Xiao

Received: 10 March 2014 / Revised: 18 August 2014 / Accepted: 26 August 2014 / Published online: 16 September 2014

Abstract The structural changes of bovine serum albumin (BSA) under high-intensity ultrasonication were investigated by fluorescence spectroscopy and mass spectrometry. Evidence for the ultrasonication-induced conformational changes of BSA was provided by the intensity changes and maximum-wavelength shift in fluorescence spectrometry. Matrix-assisted laser desorption–ionization time-of-flight mass spectroscopy (MALDI-TOF MS) revealed the increased intensity of the peak at the charge state +5 and a newly emerged peak at charge state +6, indicating that the protein became unfolded after ultrasonication. Prevalent unfolding of BSA after ultrasonication was revealed by hydrogen–deuterium exchange coupled with mass spectrometry (HDX-MS). Increased intensity and duration of ultrasonication further promoted the unfolding of the protein. The unfolding induced by ultrasonication goes through an intermediate state similar to that induced by a low concentration of denaturant.

Keywords BSA structure · Ultrasound · H–D exchange · Mass spectrometry

Q. Zhang · Z. Tu (✉) · H. Wang · X. Sha
State Key Laboratory of Food Science and Technology, Nanchang University, Nanchang, Jiangxi 330047, China
e-mail: Tuzc_mail@aliyun.com

Z. Tu · X. Huang
College of Life Science, Jiangxi Normal University, Nanchang, Jiangxi 330022, China

H. Wang
Engineering Research Center for Biomass Conversion, Ministry of Education, Nanchang University, Nanchang, Jiangxi 330047, China

H. Xiao (✉)
Department of Pathology, Albert Einstein College of Medicine, Yeshiva University, Bronx, New York, NY 10461, USA
e-mail: hui.xiao@einstein.yu.edu

Introduction

Ultrasound has become an important technique widely used in food processing. The ultrasound waves absorbed by food can induce alterations in the protein structure, including loss of the secondary structure, formation of new intra and inter-molecular interactions, disulfide-bond rearrangements, and conformational changes [1]. The effects of ultrasound mainly result from acoustic cavitation: the formation, growth, and implosive collapse of bubbles in the liquid, which generates intense local heating and high pressure [2]. The heat generated in ultrasonic processing is the major factor affecting the protein structure. The thermal aggregation process of the model protein BSA has been observed [3]. Stathopulos et al. reported that ultrasonication induced the conversion of the α-helix to a β-sheet, especially in the proteins containing the most α-helical structures [4]. However, results have been revealed to vary with temperature: the α-helix content of BSA was increased after ultrasonication with the temperature maintained at 2 °C, whereas it was significantly reduced when the temperature was maintained at 85 °C [5, 6].

The main interest of the pharmaceutical and food industry is the functional properties of proteins, including kinesthetic, organoleptic, hydration, interfacial, enzymatic, and rheological properties. These properties are affected by the structural changes occurring under ultrasonication. Gulseren et al. studied the effect of high-intensity ultrasound on the structure and functionality of BSA and found that ultrasound increased the surface activity, surface hydrophobicity, and surface charge of the protein [5]. Given that high-intensity ultrasound alters the protein structures, one would expect alterations in both protein structure and function upon ultrasonication. However, the results after application of

ultrasonication are varied; for example, a 70 % reduction in glucose-6-phosphate dehydrogenase activity upon ultrasonication was observed by Ozbek and Ulgen, whereas the activity of alkaline phosphatase under the same conditions remained unchanged [7]. This emphasizes the importance of understanding the physicochemical effects of ultrasound on proteins. Traditionally, structural changes of protein are measured by circular dichroism [8], fluorescent spectrometry [9], and Fourier-transform infrared spectroscopy [10]. However, these methods can only provide global structural information, without revealing what exactly happened inside the protein and which area of the protein was changed. Knowledge of the effect of ultrasound on the structural and functional properties of proteins has therefore been hindered by the lack of detailed structural information. To better understand the structure–function relationship, a detailed protein mapping is desired.

Hydrogen–deuterium exchange coupled to mass spectrometry (HDX-MS) can be used to determine the localization of secondary structure elements, binding sites, and conformational changes of proteins in solution [11, 12]. Complementary to the traditionally biophysical methods for structural studies, HDX-MS provides substantial evidence of protein structural changes at the peptide level with a minimum amount of sample [13, 14]. A reduced HDX rate for a region indicates that either the peptide is involved with interactions or the region has become more folded, and vice versa. Presumably, when the protein structure is disrupted by ultrasonication in a specific area, the changes can be reflected by the altered HDX rate.

In this work, BSA was ultrasonicated at two different ultrasound intensities (75 W cm^{-2} and 150 W cm^{-2}) with varying duration. We monitored the structural changes of BSA using fluorescence spectroscopy and mass spectrometry. We revealed that ultrasound induced conformational changes of BSA. The deuterium incorporation of ultrasonicated BSA increased significantly compared with that of unsonicated BSA, especially for high-intensity ultrasonication.

Experimental

Materials

Bovine serum albumin (BSA), pepsin, urea, citric acid, sinapic acid, acetone, and formic acid (FA) were purchased from Sigma Chemical Co. (St. Louis, MO). Deuterium oxide (99 %) was purchased from Cambridge Isotope Laboratories, Inc. (Waltham, MA). Tris (2-carboxyethyl) phosphine (TCEP) was obtained from Fisher Scientific Pierce (Waltham, CA). All solutions were prepared with deionized water (Milli-Q, Millipore Corporation). All other reagents used were of analytical grade.

Ultrasonicated sample preparation

BSA (0.5 g) was dissolved in 50 mL 50 mmol L^{-1} sodium-phosphate buffer at pH 7.4. The solution was split into four aliquots. One aliquot BSA was used as the control. The other BSA solutions were treated by a probe sonicator (Model 550 Sonic Dismembrator, Fisher Scientific, Pittsburgh, PA, 20 kHz) equipped with a microtip probe (1/8"=3.2 mm). In this sonicator setup, the actual minimum ultrasonic intensity was 75 W cm^{-2} and the maximum intensity was 150 W cm^{-2}. The sample tube was kept in an ice bath at atmospheric pressure. The probe was immersed in the sample solution. The solution was treated by ultrasound with a 5 s-on-and-5 s-off pulsation, using three different conditions:

1. actual ultrasound intensity at 75 W cm^{-2} for 5 min;
2. actual ultrasound intensity at 150 W cm^{-2} for 5 min; and
3. actual ultrasound intensity at 150 W cm^{-2} for 10 min.

The samples were stored at 4 °C until further analysis. All the subsequent analyses were performed within 24 h after the sonication.

Fluorescence spectrometry

The intrinsic emission-fluorescence spectra of the protein samples (10 mg mL^{-1} in 50 mmol L^{-1} pH 7.4 phosphate buffer) were obtained by a Perkin-Elmer LS-5 fluorescence spectrophotometer (Perkin-Elmer Corp.). To minimize the contribution of tyrosine residues to the emission spectra, the protein solutions were excited at 280 nm, and emission spectra were recorded from 300 to 500 nm at a constant slit width of 2 nm for both excitation and emission. All measurements were conducted in triplicate.

MALDI-TOF mass-spectrometry analysis

Mass-spectrometry analysis was performed using a 4800 MALDI TOF-TOF mass spectrometer (AB Sciex, Framingham, MA) equipped with a 335 nm Nd:YAG laser with a 200 Hz firing rate. MS spectra were acquired with 20 laser shots per sub-spectrum at an intensity of 6300 arbitrary units, with a bin size of 20 ns, in linear positive-ion mode. An average of 60 sub-spectra with 1500 total shots were used to obtain each MS spectrum to ensure a better S/N ratio. Sinapic acid (10 mg mL^{-1}) in 50 % acetonitrile–50 % Tris–HCl (10 mmol L^{-1} pH 7.0) was used as the matrix. The proteins were mixed 1:1 with the matrix, and then 1.5 μL mixture was spotted onto the MALDI target and air dried before analysis. Each sample was spotted on at least three individual target

positions, and each spot was recorded at a mass range from 8000 to 200,000 Da.

Hydrogen–deuterium exchange and mass spectrometry

HDX-MS experiments were performed as depicted in the workflow scheme (Fig. 1). Different sonicated BSA solution samples (2 μL, 10 μg μL^{-1}) were diluted 10 times into D_2O in an ice-water bath. After 10 min, the deuterium exchange was quenched with an equal volume of prechilled quenching buffer (0.5 mol L^{-1} citric acid, 0 °C, pH 2.2) containing 6 mol L^{-1} urea and 100 mmol L^{-1} TCEP. Pepsin (5 μL, 2 mg mL^{-1}, 0.05 mol L^{-1} HCl) was added immediately to digest the protein at room temperature for 4 min. The solution (45 μL) was then injected onto a 50×1.00 mm C18 column (Phenomenex) on a Shimadzu HPLC with LC-10AD pumps. The solvent PEEK tubing, injector, and HPLC column were submerged in an ice-water bath to minimize back-exchange.

Solvent A was 5 % acetonitrile with 0.1 % FA, and solvent B was 95 % acetonitrile with 0.1 % FA. After desalting for 5 min with 5 % solvent B, the samples were eluted with a 5–15 % gradient for 1 min and 15–50 % gradient for 10 min at 50 μL min^{-1}. The eluent was directly delivered into an LTQ-Orbitrap Velos mass spectrometer (Thermo Fisher Scientific) for mass-spectrometry analysis. For peptic peptide identification, the mass spectrometer was operated in a data-dependent MS–MS mode. The normalized collision energy was set to 28 % for collision-induced dissociation (CID). The signal threshold for initiating an MS–MS event was set to 500 counts. Charge-state screening was enabled, and precursors with unknown charge state were excluded. Dynamic exclusion was enabled, with an exclusion duration of 90 s. All the HDX experiments were performed in triplicate.

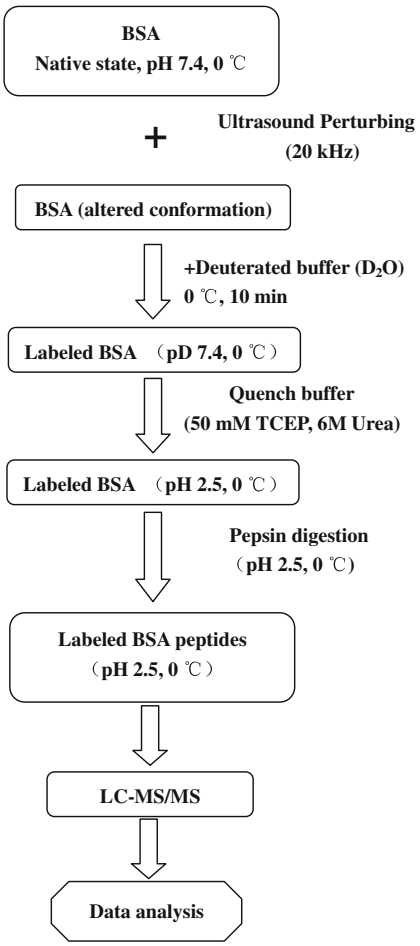

Fig. 1 Schematic depiction of the work flow of HDX-MS of BSA

Data analysis

The peptic peptides were identified by Sequest searching against the bovine serum albumin (P02769). The HDX-MS data were analyzed by the EX-MS software [15]. Average changes in deuterium incorporation (ΔHDX)±S.D. were determined from three separate experiments. The changes in deuterium incorporation (ΔHDX) were defined as the difference between the average values of the ultrasonicated BSA and the native BSA. Difference in deuteration in each domain was calculated by summing the ΔHDX value of all included peptides and dividing by the total number of amino-acid residues.

Results and discussion

Intrinsic-fluorescence spectra

The fluorescence spectra of BSA with or without different ultrasound treatments are shown in Fig. 2. The native BSA has a strong fluorescence-emission peak at 348 nm after being

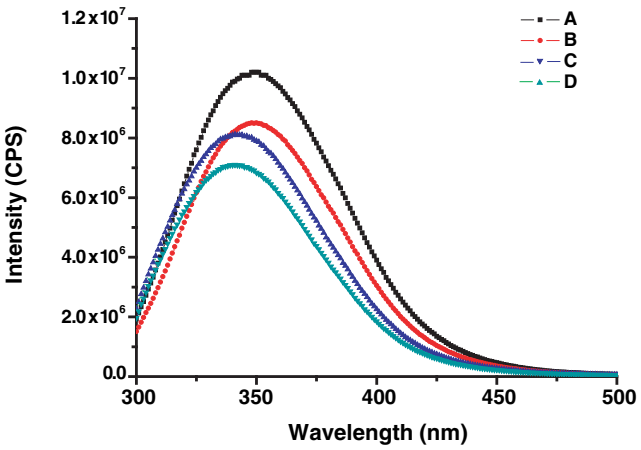

Fig. 2 Fluorescence spectra of BSA under different ultrasonication conditions: *A*: native BSA, *B*: 75 W cm^{-2} for 5 min, *C*: 150 W cm^{-2} for 5 min, and *D*: 150 W cm^{-2} for 10 min. The excitation wavelength is 280 nm

excited at the wavelength of 280 nm. The fluorescence intensity of BSA ultrasonicated at 75 W cm^{-2} for 5 min was reduced markedly, but no maximum-emission wavelength shift was observed. When the higher intensity of ultrasonication, 150 W cm^{-2} for 5 min, was applied, the fluorescence intensity was further reduced. In addition, a blue shift of the emission maxima from 348 to 341 nm was observed. Extended time under this ultrasonication intensity induced an additional reduction of the fluorescence intensity, with no extra blue shift of the emission maxima. The fluorescence quenching is indicative of exposure of the protein hydrophobic regions to the solvent [16, 17]. In BSA, tryptophan (Trp) is the major contributor of the intrinsic fluorescence, whereas the other possible fluorophores, Phe and Tyr, contribute little because of the low quantum yield and complete quenching by nearby amino-acid residues, respectively [18]. A closer look at the structure of BSA reveals that, of two of the tryptophans contained in BSA, Trp 134 is more exposed to a hydrophilic environment, whereas Trp 213 is deeply buried in the hydrophobic loop [19]. Trp 213 is often used as the fluorescence probe to monitor the quenching effect with a variety of ligands because it is the fluorophore involved in hydrophobic ligand binding as a result of its hydrophobic environment [17]. The blue shift has also been observed at low GuHCl concentrations in GuHCl-induced denaturation of BSA and HSA [20, 21]. Togashi et al. attribute this to the rearrangement of domain II, through which the residue Trp 213 moves to a less-polar, inner core of the hydrophobic cavity in domain II [22]. However, this alone does not explain the simultaneous blue shift and fluorescence-intensity reduction observed in our ultrasonication-induced protein denaturation. Given ultrasonication is the only treatment in our experimental method, the most probable cause of the reduced intensity and the blue shift is the protein structural changes. The protein underwent a structural rearrangement resulting in a more open conformation in the vicinity of Trp 134 or Trp 213, as indicated by the quenched fluorescence. However, the blue shift is indicative of an increased hydrophobicity in the proximity of the tryptophan, which is contradicted by the more open structural arrangement. A reasonable explanation for this is that two of the tryptophan residues reacted differently in response to the structural perturbation by ultrasonication, with one more exposed to the solvent, causing fluorescence quenching, and the other one more shielded from the solvent, leading to a blue shift of the emission maxima. To better understand the detailed structural changes induced by ultrasonication, we used mass-spectrometry-based methods, measuring the charge-state distribution by use of MALDI-TOF and monitoring local structural changes by use of HDX-MS.

Average molecular weight and charge-state distribution

During ultrasonication it is crucial to control the temperature, because the heat generated by ultrasonication will induce thermal aggregation of proteins. The ultrasonication conditions we used included a temperature maintained at 0 °C, under which thermal aggregation is minimal [3]. To ensure that BSA did not aggregate under the ultrasonication conditions applied to the protein, the samples were subjected to MALDI-TOF MS determination. The mass spectra of BSA before and after ultrasonication are shown in Fig. 3. The molecular weight of BSA was maintained at 66 kDa, indicating no modification caused by ultrasonication. Importantly, there was no trimer and no other oligomer observed under any of our temperature-controlled ultrasonication conditions (Fig. 3). Also, there was no significant change to the dimer peak at 133 kDa, indicating no thermal aggregation induced by ultrasonication. The charge state +2 peak, represented by the peak at 33.2 kDa, changed little. The higher charge state, however, had obvious changes after ultrasonication, particularly at the higher intensity. The relative intensity of the charge state +5 peak (represented by the peak at ~13.5 kDa) of BSA treated with the higher ultrasound intensity (150 W cm^{-2}) was much higher than that of BSA that was untreated or was treated with a lower ultrasound intensity (Fig. 3). The charge state +6 peak (represented by the peak at ~10 kDa) was present only after higher intensity ultrasonication (Fig. 3c, d).

Monitoring the changes in charge-state distributions of protein ions in electrospray-ionization mass spectra is one of the commonly accepted tools for detecting large-scale conformational changes of proteins in solution [23, 24]. The relative abundances of the signals usually reflect some distribution of ion stability which is indicative of protein conformation [23]. It is not uncommon to observe multiple charged ions of protein in MALDI-TOF mass spectra [25, 26]. The appearance of the higher-charge-state +6 protein ions and increased peak intensity of +5 protein ions indicate that BSA conformational stability was disturbed by high-intensity ultrasonication. It should be noted that the matrix we used was sinapic acid dissolved in Tris–HCl at pH 8.0, which is suitable for detection of non-covalent complexes. We did not use trifluoroacetic acid (TFA), to avoid its detrimental effect on dimer, trimer, or other oligomer observations of the protein.

Local structural changes determined by HDX-MS

To investigate exactly what occurred during ultrasonic treatment, HDX-MS was performed on the ultrasonicated protein samples and compared with results for the sample before ultrasonication. Because there are 17 pairs of disulfide bonds in BSA [27], urea and the reducing agent, TCEP, were used to assist pepsin digestion. EXMS program coupled with manual checks was used to analyze the HDX-MS data [15]. In total, 34 peptides were consistently detected providing 94 % sequence coverage of this protein containing 583 amino-acid residues. Figure 4a summarizes the effect of ultrasound treatments of 75 W cm^{-2} for 5 min and 150 W cm^{-2} for 5 and

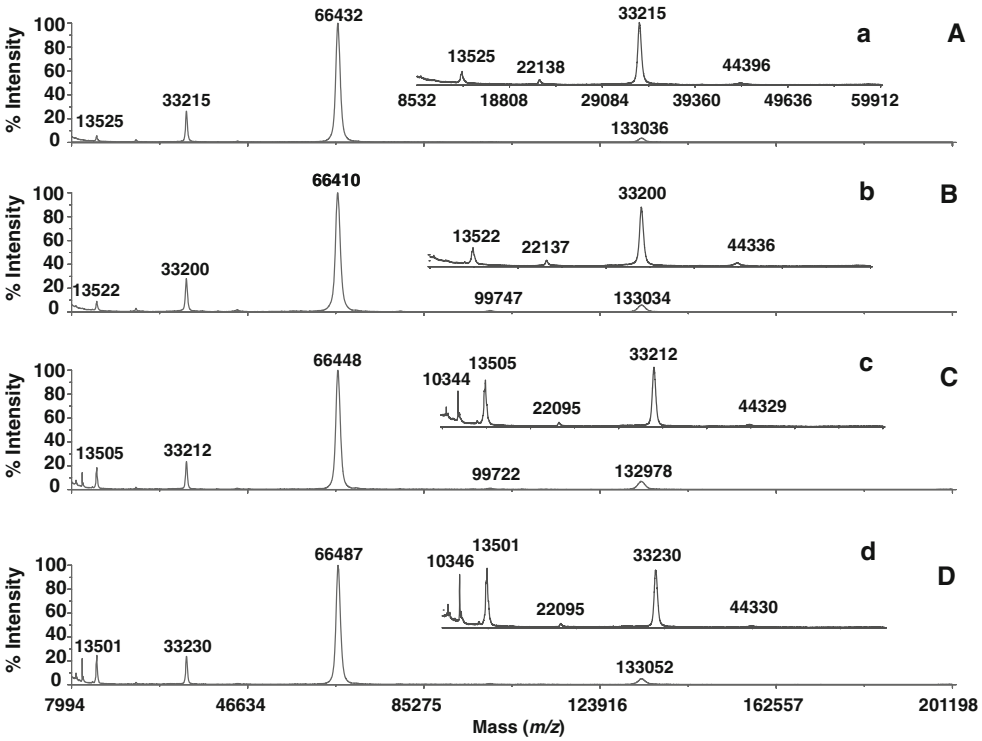

Fig. 3 MALDI-TOF-MS analysis of BSA under different ultrasonication conditions: *A*: native BSA, *B*: 75 W cm^{-2} for 5 min, *C*: 150 W cm^{-2} for 5 min, and *D*: 150 W cm^{-2} for 10 min

10 min on BSA deuterium incorporation. The difference in deuterium incorporation for each peptide corresponds to the difference between the centroid values of the mass distribution of the peptides from normal BSA and ultrasonicated BSA.

Increased deuterium incorporation was observed for most peptides after ultrasonication at 75 W cm^{-2} for 5 min (Fig. 4a, series A). However, the degree of the deuterium incorporation was quite low, with the highest deuterium incorporation being 1.33 Da in peptide 488–505 (ΔHDX). Given the number of amino-acid residues of this peptide is 17, the deuterium incorporation per amino acid (ΔHDX/AA) is only 0.078 mu. This suggests that the ultrasonication at 75 W cm^{-2} for 5 min did disturb the protein structure, but to a very small extent. When the ultrasonication intensity was increased to 150 W cm^{-2}, the deuterium incorporation for most peptides was significantly increased, indicating that the structure of the protein was disturbed to a greater degree (Fig. 4a, series B). In addition, the increased duration of ultrasonication also contributed greatly to disrupting the protein structure, as evidenced by the overall increased deuterium incorporation (Fig. 4a, series C). This agrees with Guzey et al.'s observation, in which ultrasound was found to reduce the helical content of BSA, e.g. from 61 % for native protein to 40 % for sonicated proteins at 85 °C [6]. When this type of ultrasonically-induced change to the molecular structure of BSA occurs, deuterium incorporation will be accelerated because of the loss of the secondary structure.

BSA comprises three domains (I, II, and III), which contain residues 1–184 (domain I), residues 185–377 (domain II), and residues 378–583 (domain III) [27, 28]. These three domains, together with 17 disulfide bridges, form a V-shape structure. The deuterium incorporation per amino acid was calculated for each domain and is summarized in Fig. 4b. Under all three conditions, ΔHDX values of peptides in domain III were highest, whereas those in domain I and II were much lower, suggesting that the BSA structure was perturbed by ultrasonication to a different degree in its three domains. The results suggest that domain III was the most perturbed region, whereas domain I and domain II were much less affected. In a recent study of local unfolding of BSA using steady-state and time-resolved fluorescence spectroscopy, Togashi et al. revealed that BSA denaturation induced by guanidinium hydrochloride (GuHCl) involves a two-stage process, with the formation of an intermediate state. The first stage involves the denaturation of domain III, whereas the second stage involves the denaturation of domain II [22]. Similarly, using two fluorescence probes bound to domains II and III of human serum albumin (HSA), Tanaka et al. revealed that the structure of domain III is unfolded in the initial stages of pressure-induced denaturation, whereas the structure of domain II is unaffected [29]. Our results are also in agreement with the well-designed unfolding study of HSA by Ahmad et al., in which four probes were used to enable all three domains to be monitored. Their results revealed that the order of stability of the three domains is domain I > domain II > domain III [30].

The unfolding energy for each domain of HSA is 7.4, 4.4, and 1.4 kcal mol^{-1} for domain I, II, and III, respectively [30]. Because of the energy barrier, unfolding induced by

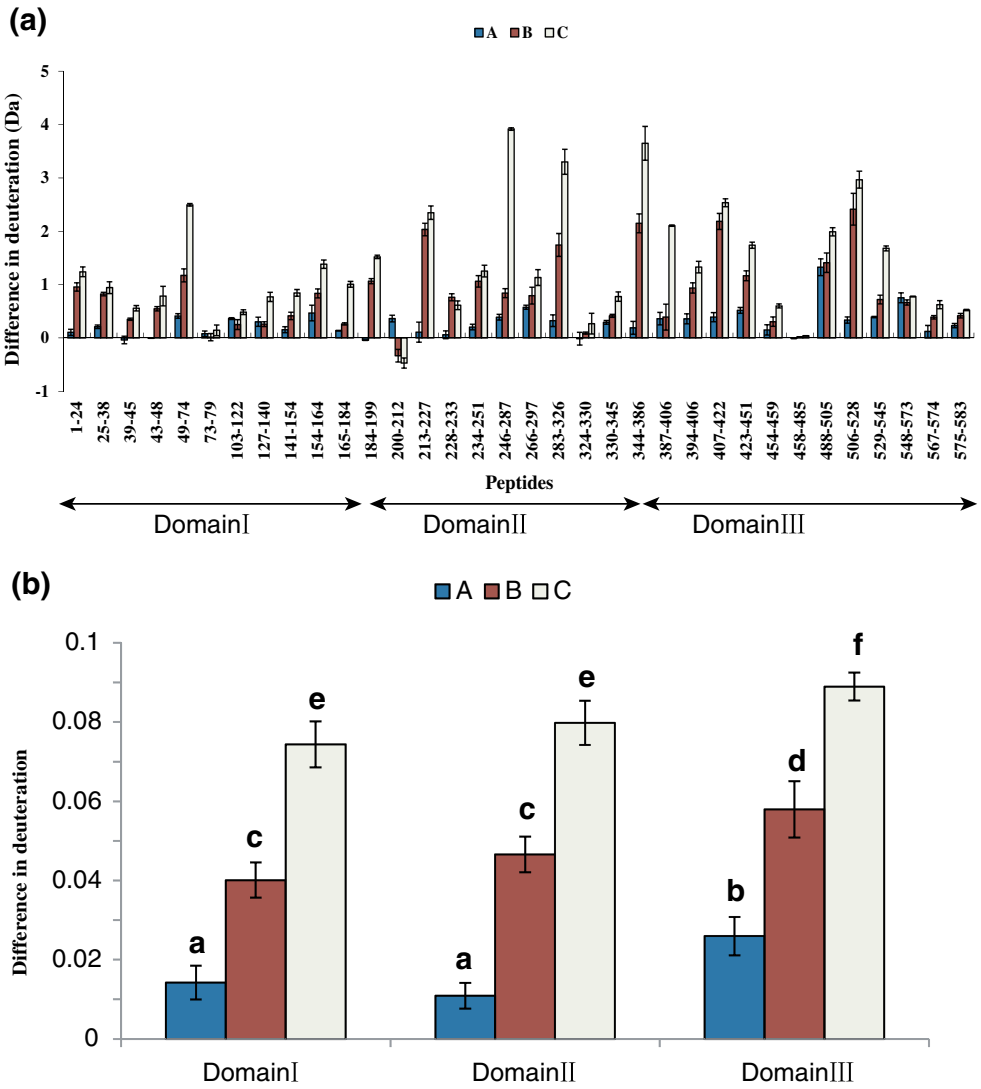

Fig. 4 Ultrasonication-induced alterations in deuteration, referenced against the native BSA, under various ultrasonication conditions: (**a**) peptides and (**b**) domains. Data denote the mean±SD of three separate experiments. Differences in deuteration per peptide (ΔHDX) are expressed in Da. Peptides are labeled with the corresponding amino-acid numbers. Difference in deuteration in each domain was calculated by summing the ΔHDX value of all included peptides and normalized by the total number of amino-acid residues. *A*: 75 W cm^{-2} for 5 min, *B*: 150 W cm^{-2} for 5 min, and *C*: 150 W cm^{-2} for 10 min

denaturant or pressure is usually associated with a multistage process with intermediate state(s). Surprisingly, when the ultrasonication of 75 W cm^{-2} was applied to BSA for 5 min, most peptides had increased deuterium incorporation, indicating a more flexible conformation induced by ultrasonication. Unlike partial unfolding induced by low concentrations of denaturant, ultrasonication at this intensity induced conformational changes in all three domains. It has been revealed that ultrasonication can significantly change protein structures [31, 32]. When proteins are subjected to ultrasonic treatment, the force of the cavitation generated by ultrasonication can increase the surface charge and surface activity of BSA [33]. Our HDX-MS results revealed that, with the 5 min at 75 W cm^{-2} ultrasonication, the cavitation force is strong enough to disturb the structure of all three domains, leading to the overall increased deuterium incorporation in all three domains. Noticeably, some regions were disturbed to a lesser degree, as indicated by those peptides undergoing little change under this treatment, including peptides 1–24, 39–45, 43–48, and 73–79 in domain I, 184–199, 213–227, 228–233, and 324–330 in domain II, and 458–485 in domain III (Fig. 4a, series A). This can be attributed to the location and the secondary structure of these peptides. All these peptides are α-helix peptides, and are located in the core of each domain that may not be easily disturbed by light ultrasonication. In contrast, because peptide 488–505 is composed mainly of a loop and located outside the protein, it was strongly perturbed by 5 min of 75 W cm^{-2} ultrasonication.

When the stronger ultrasonication, 5 min of 150 W cm^{-2}, was applied to the protein, most of the peptides had increased deuterium incorporation, indicating the protein adopted a more unfolded conformation (Fig. 4a, series B, and b series B). The additional duration (10 min of 150 W cm^{-2}) of ultrasonication promoted the deuterium incorporation of the protein (Fig. 4a, series C and b series C), indicative of a further-unfolded protein conformation. Again, this extra unfolding caused by stronger ultrasonication was not limited to a specific domain but affected all three domains of BSA, as

reflected by an overall increased level of deuteration in all three domains. Interestingly, the peptide 200–212 underwent the opposite effect under the stronger ultrasonic treatment (Fig. 4a), with its deuterium incorporation reducing instead of increasing. To avoid possible errors from data analysis, the mass spectra of this peptide under all conditions were fitted with a Gaussian function; the centroids calculated are shown by the arrows in Fig. 5. The reduced deuterium incorporation suggests that this region of the protein assumed a more compact conformation compared with its native state. As a comparison, the mass spectra of the neighboring peptides, for example 184–199, revealed a clear mass increase upon ultrasonication (Fig. 4a). The sharp change of deuterium level in peptide 200–212 suggests that the protein underwent a structural rearrangement, through which the protein may reach an intermediate state. A closer look at this peptide in the context of the protein's 3D structure revealed that the peptide is located right beside Trp 213 (Fig. 6), which is one of the fluorophores responsible for fluorescence emission in Fig. 2. As discussed earlier, the blue shift in fluorescence spectra suggested ultrasonication at 150 W cm^{-2} forced the protein to adopt a conformation in which Trp 213 was shielded from the solvent. The reduced deuterium levels in the immediate vicinity of this amino acid strongly support this notion. Furthermore, two neighboring peptides in the 3D structure, peptide 324–330 and 458–485 (Figs. 4a and 6, blue colored), had almost unchanged deuterium levels under the stronger ultrasonication. The prolonged ultrasonication time at 150 W cm^{-2} (10 min) did not alter the deuterium level of the peptide, suggesting there were no further significant structural changes in this region, which is consistent with the observation of no wavelength shift in the fluorescence emission

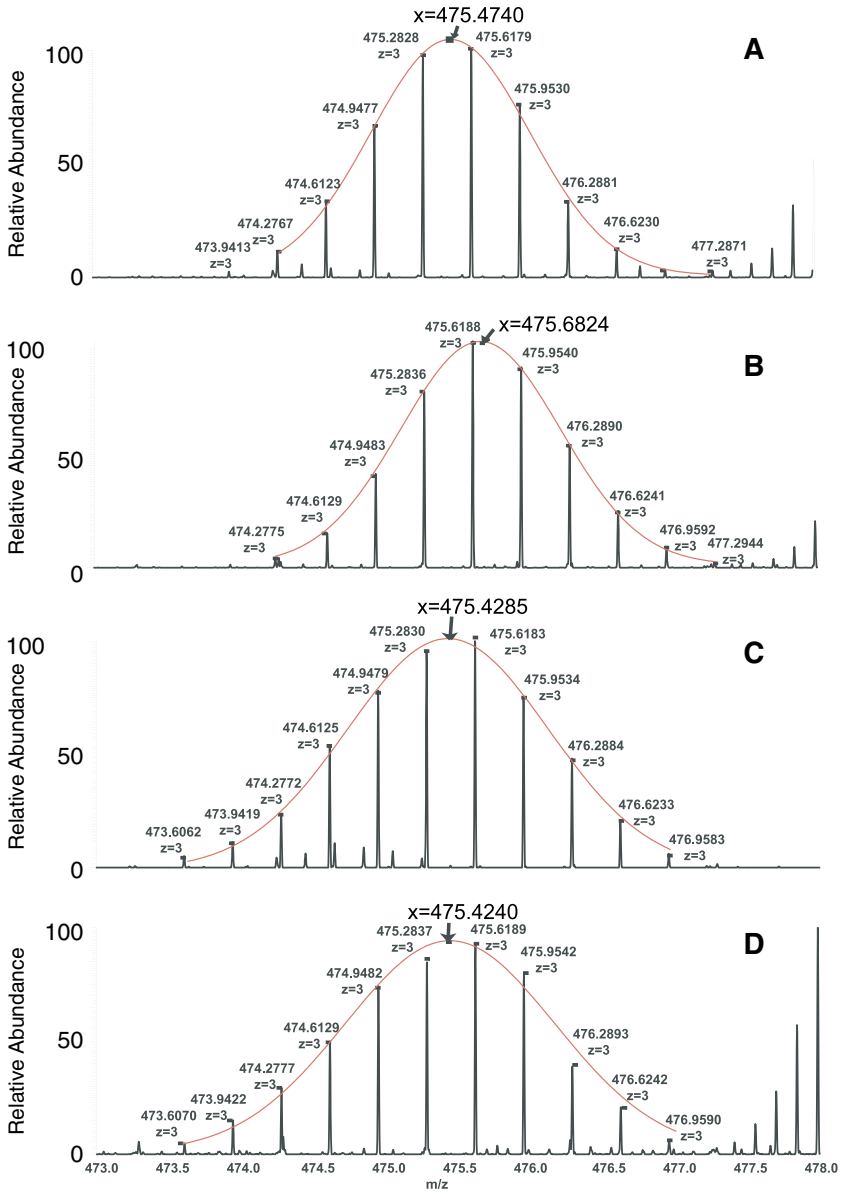

Fig. 5 Deuterated mass spectra of peptide 200–212 under different ultrasonication conditions: (**a**) native BSA, (**b**) 75 W cm^{-2} for 5 min, (**c**) 150 W cm^{-2} for 5 min, and (**d**) 150 W cm^{-2} for 10 min. The centroid of each mass spectrum was obtained by fitting the curve using a Gaussian function

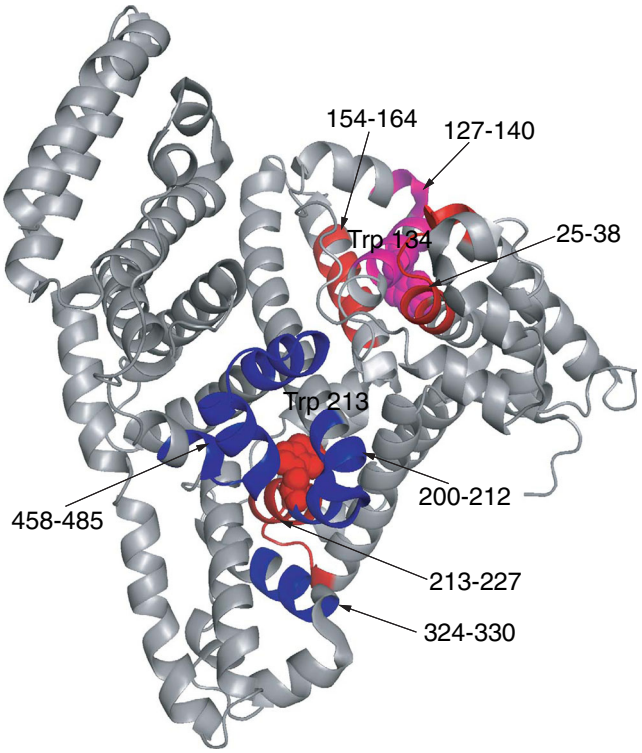

Fig. 6 Mapping local HDX alterations in the vicinity of Trp 134 and Trp 213 (PDB code IJTI). Trp 134 and Trp 213 are shown as *pink spheres* and *red spheres*, respectively. Peptide 127–140 containing Trp 134 is colored *pink*. The neighboring peptides are color-coded as follows: *pink* and *red* = increase in deuterium incorporation (ΔHDX>0), peptide 127–140, 25–38, 154–164, and 213–227; *blue* = no change in deuterium incorporation (ΔHDX≤0), peptide 200–212, 324–330, and 458–485

(Fig. 2c, d). These three peptides formed a stable neighborhood that resisted structural perturbation caused by ultrasonication. It should be noted our HDX-MS is limited to the peptide level; the HDX information in a single residue is not attainable. Although peptide 213–227 had a significantly increased deuterium level, the increase could be mainly contributed by the loop of this peptide.

From Fig. 2, the intensity of the fluorescence was reduced when longer ultrasonication was applied. This is also in agreement with the changes in deuterium level of the peptide containing Trp 134. The deuterium level of peptide 127–140 was more than doubled with the extended ultrasonication time, indicating a more unfolded structure in this region leading to fluorescence quenching. This structural change was also supported by the changes in its neighboring peptides; for example, the peptides 25–38 and 154–164 (Figs. 4a and 6, red colored) had significantly increased deuterium labeling.

The apparently different HDX behavior in domain II suggests that, similarly to denaturant-induced unfolding, unfolding induced by ultrasonication also goes through an intermediate state. Our HDX-MS results, however, revealed that the ultrasonication-induced unfolding is different from that induced by denaturants. Our results revealed that it was domain II that maintained the relatively stable core of the protein. The intrinsic-fluorescence probe, Trp213, is located in this region, and therefore has a reduced deuteration level and a blue shift. Compared with the guanidine-hydrochloride (GuHCl)-induced denaturation, it is likely that the denaturation induced by ultrasonication was still in the early stage. At a relatively low concentration of GuHCl (below 2 mol L^{-1}), BSA was found to have a blue shift and a reduced fluorescence signal [22]. Further addition of the denaturant (>2 mol L^{-1}) gives the protein a red shift with a further reduction in fluorescence signal, indicating a very open conformation. With 10 min of the maximum intensity (i.e., 150 W cm^{-2}) ultrasonication, the fluorescence spectra were similar to those obtained after the denaturation induced by the low concentration of GuHCl, indicating a relatively small structural perturbation. With higher ultrasonication intensity, it is expected that the protein undergoes this unfolding process to a much higher degree. This trend can be seen from Fig. 4a, b, because the deuteration of each domain significantly increases with increased intensity and duration of the ultrasonication.

It should be noted that the fluorescence studies relied on those fluorescent probes binding to specific sites of the protein [29, 30]. The probes can monitor any conformational changes occurring in the near vicinity of the probes; however, they may not be able to observe the conformational changes of distal sites, in particular subtle conformational changes. Therefore, HDX-MS provides not only a more detailed but also a more sensitive method of monitoring conformational changes of proteins. Despite the great difference between the ultrasonication-induced changes and denaturant-induced changes, both had similar domain changes, providing evidence of the existence of the intermediate state.

Conclusions

We used fluorescence spectroscopy and mass spectrometry to probe the structural changes of BSA induced by high-intensity ultrasonication. The intensity changes and maximum-wavelength shift observed in the fluorescence spectrometry are well explained by HDX-MS results. The high-intensity ultrasonication unfolded BSA throughout all regions of the protein. The unfolding of the protein is dependent on the intensity and duration of ultrasonication. The HDX-MS results suggest that the unfolding induced by ultrasonication goes through an intermediate state similar to that induced by a low concentration of denaturant.

Acknowledgments This study was supported by National High Technology Research and Development Program of China (863 Program, No. 2013AA102205), National Program on Key Basic Research Project (No.2012CB126314), and Key Project for Science and Technology Innovation of Jiangxi Province (20124ACB00600).

References

1. Pavlovskaya G, McClements D, Povey M (1992) Ultrasonic investigation of aqueous solutions of a globular protein. Food Hydrocoll 6(3):253–262. doi:10.1016/S0268-005X(09)80093-3
2. Suslick KS, Didenko Y, Fang MM, Hyeon T, Kolbeck KJ, McNamara WB, Mdleleni MM, Wong M (1999) Acoustic cavitation and its chemical consequences. Philos Trans R Soc London, Ser A 357(1751):335–353. doi:10.1098/rsta.1999.0330
3. Militello V, Vetri V, Leone M (2003) Conformational changes involved in thermal aggregation processes of bovine serum albumin. Biophys Chem 105(1):133–141. doi:10.1016/s0301-4622(03)00153-4
4. Stathopulos PB, Scholz GA, Hwang YM, Rumfeldt JAO, Lepock JR, Meiering EM (2004) Sonication of proteins causes formation of aggregates that resemble amyloid. Protein Sci 13(11):3017–3027. doi:10.1110/Ps.04831804
5. Gulseren I, Guzey D, Bruce BD, Weiss J (2007) Structural and functional changes in ultrasonicated bovine serum albumin solutions. Ultrason Sonochem 14(2):173–183. doi:10.1016/j.ultsonch.2005.07.006
6. Guzey D, Gulseren I, Bruce B, Weiss J (2006) Interfacial properties and structural conformation of thermosonicated bovine serum albumin. Food Hydrocoll 20(5):669–677. doi:10.1016/j.foodhyd.2005.06.008
7. Özbek B, Ülgen K Ö. (2000) The stability of enzymes after sonication. Process Biochem 35(9):1037–1043. doi:10.1016/S0032-9592(00)00141-2
8. Day L, Zhai J, Xu M, Jones NC, Hoffmann SV, Wooster TJ (2014) Conformational changes of globular proteins adsorbed at oil-in-water emulsion interfaces examined by Synchrotron Radiation Circular Dichroism. Food Hydrocoll 34:78–87. doi:10.1016/j.foodhyd.2012.12.015
9. Togashi DM, Ryder AG (2006) Time-resolved fluorescence studies on bovine serum albumin denaturation process. J Fluoresc 16(2):153–160. doi:10.1007/s10895-005-0029-9
10. Murayama K, Tomida M (2004) Heat-induced secondary structure and conformation change of bovine serum albumin investigated by Fourier transform infrared spectroscopy. Biochemistry-Us 43(36):11526–11532. doi:10.1021/Bi0489154
11. Landreh M, Astorga-Wells J, Johansson J, Bergman T, Jornvall H (2011) New developments in protein structure-function analysis by MS and use of hydrogen-deuterium exchange microfluidics. FEBS J 278(20):3815–3821. doi:10.1111/j.1742-4658.2011.08215.x
12. Michalski A, Damoc E, Lange O, Denisov E, Nolting D, Muller M, Viner R, Schwartz J, Remes P, Belford M, Dunyach JJ, Cox J, Horning S, Mann M, Makarov A (2012) Ultra high resolution linear ion trap orbitrap mass spectrometer (orbitrap elite) facilitates top down LC MS/MS and versatile peptide fragmentation modes. Mol Cell Proteomics 11(3). doi:10.1074/mcp.O111.013698
13. Marcsisin SR, Engen JR (2010) Hydrogen exchange mass spectrometry: what is it and what can it tell us? Anal Biol Chem 397(3):967–972. doi:10.1007/s00216-010-3556-4
14. Wales TE, Engen JR (2006) Hydrogen exchange mass spectrometry for the analysis of protein dynamics. Mass Spectrom Rev 25(1):158–170. doi:10.1002/mas.20064
15. Kan ZY, Mayne L, Chetty PS, Englander SW (2011) ExMS: data analysis for HX-MS experiments. J Am Soc Mass Spectrom 22(11):1906–1915. doi:10.1007/s13361-011-0236-3
16. Semisotnov GV, Rodionova NA, Razgulyaev OI, Uversky VN, Gripas AF, Gilmanshin RI (1991) Study of the "molten globule" intermediate state in protein folding by a hydrophobic fluorescent probe. Biopolymers 31(1):119–128. doi:10.1002/bip.360310111
17. Sułkowska A (2002) Interaction of drugs with bovine and human serum albumin. J Mol Struct 614(1):227–232. doi:10.1016/S0022-2860(02)00256-9
18. Peters T Jr (1985) Serum albumin. Adv Protein Chem 37:161–245. doi:10.1016/S0065-3233(08)60065-0
19. Papadopoulou A, Green RJ, Frazier RA (2005) Interaction of flavonoids with bovine serum albumin: a fluorescence quenching study. J Agric Food Chem 53(1):158–163. doi:10.1021/jf048693g
20. Sułkowska A, Rownicka J, Bojko B, Pożycka J, Zubik-Skupień I, Sułkowski W (2004) Effect of guanidine hydrochloride on bovine serum albumin complex with antithyroid drugs: fluorescence study. J Mol Struct 704(1):291–295. doi:10.1016/j.molstruc.2003.12.065
21. Flora K, Brennan JD, Baker GA, Doody MA, Bright FV (1998) Unfolding of acrylodan-labeled human serum albumin probed by steady-state and time-resolved fluorescence methods. Biophys J 75(2):1084–1096. doi:10.1016/S0006-3495(98)77598-8
22. Togashi DM, Ryder AG, O'Shaughnessy D (2010) Monitoring local unfolding of bovine serum albumin during denaturation using steady-state and time-resolved fluorescence spectroscopy. J Fluoresc 20(2):441–452. doi:10.1007/s10895-009-0566-8
23. Loo JA, Loo RR, Udseth HR, Edmonds CG, Smith RD (1991) Solvent-induced conformational changes of polypeptides probed by electrospray-ionization mass spectrometry. Rapid Commun Mass Spectrom: RCM 5(3):101–105. doi:10.1002/rcm.1290050303
24. Dobo A, Kaltashov IA (2001) Detection of multiple protein conformational ensembles in solution via deconvolution of charge-state distributions in ESI MS. Anal Chem 73(20):4763–4773. doi:10.1021/ac010713f
25. Zhou J, Lee TD (1995) Charge state distribution shifting of protein ions observed in matrix-assisted laser desorption ionization mass spectrometry. J Am Soc Mass Spectrom 6(12):1183–1189. doi:10.1016/1044-0305(95)00578-1
26. Sachon E, Clodic G, Blasco T, Bolbach G (2007) Protein desolvation in UV matrix-assisted laser desorption/ionization (MALDI). J Am Soc Mass Spectrom 18(10):1880–1890. doi:10.1016/j.jasms.2007.07.029
27. Adrnlnlstratlon MSFC (1994) Structure of serum albumin. Lipoproteins Apolipoproteins Lipases 45:153–203
28. Huang X, Tu Z, Wang H, Zhang Q, Hu Y, Zhang L, Niu P, Shi Y, Xiao H (2013) Glycation promoted by dynamic high pressure microfluidisation pretreatment revealed by high resolution mass spectrometry. Food Chem 141(3):3250–3259. doi:10.1016/j.foodchem.2013.05.159
29. Tanaka N, Nishizawa H, Kunugi S (1997) Structure of pressure-induced denatured state of human serum albumin: a comparison with the intermediate in urea-induced denaturation. Biochim Biophys Acta 1338(1):13–20. doi:10.1016/S0167-4838(96)00175-6
30. Ahmad B, Ahmed MZ, Haq SK, Khan RH (2005) Guanidine hydrochloride denaturation of human serum albumin originates by local unfolding of some stable loops in domain III. Biochim Biophys Acta 1750(1):93–102. doi:10.1016/j.bbapap.2005.04.001
31. Jambrak AR, Mason TJ, Lelas V, Herceg Z, Herceg IL (2008) Effect of ultrasound treatment on solubility and foaming properties of whey protein suspensions. J Food Eng 86(2):281–287. doi:10.1016/j.jfoodeng.2007.10.004
32. Bryant CM, McClements DJ (1998) Molecular basis of protein functionality with special consideration of cold-set gels derived from heat-denatured whey. Trends Food Sci Technol 9(4):143–151. doi:10.1016/S0924-2244(98)00031-4
33. Jambrak AR, Mason TJ, Lelas V, Paniwnyk L, Herceg Z (2014) Effect of ultrasound treatment on particle size and molecular weight of whey proteins. J Food Eng 121:15–23. doi:10.1016/j.jfoodeng.2013.08.012